

Structural and Spectral Features of Complex Salts Composed of $[\text{Ni}(\text{dmit})_2]^-$ and Four- or Six-Coordination Nickel(II) Complexes of Alkyl-Substituted Cyclam

Yuji Soneta* and Kazuo Miyamura

Department of Chemistry, Faculty of Science, Tokyo University of Science,
1-3 Kagurazaka, Shinjuku-ku, Tokyo 162-8601

Received November 28, 2005; E-mail: j1304705@ed.kagu.tus.ac.jp

Slow inter-diffusion of $(\text{NBu}_4)[\text{Ni}(\text{dmit})_2]$ ($\text{dmit} = 2\text{-thioxo-1,3-dithiole-4,5-dithiolato}$) and a metal complexes ligated with alkyl-substituted cyclam, $[\text{Ni}(\text{NMe}_2\text{-dcyclam})](\text{ClO}_4)_2$ (**I**), $[\text{Ni}(\text{NMe}_2\text{-ax-dcyclam})](\text{ClO}_4)_2$ (**II**), and $[\text{Ni}(\text{NMe}_4\text{-dcyclam})]\text{Cl}_2$ (**III**), ($\text{NMe}_2\text{-dcyclam} = (1\text{RS},4\text{RS},5\text{RS},8\text{SR},11\text{SR},12\text{SR})\text{-1,5,8,12-tetramethyl-1,4,8,11-tetraazacyclotetradecane}$, $\text{NMe}_2\text{-ax-dcyclam} = (1\text{RS},4\text{RS},5\text{SR},8\text{SR},11\text{SR},12\text{RS})\text{-1,5,8,12-tetramethyl-1,4,8,11-tetraazacyclotetradecane}$, $\text{NMe}_4\text{-dcyclam} = (1\text{RS},4\text{RS},5\text{RS},8\text{SR},11\text{SR},12\text{SR})\text{-1,4,5,8,11,12-hexamethyl-1,4,8,11-tetraazacyclotetradecane}$), yielded black crystals of $[\text{Ni}(\text{NMe}_2\text{-dcyclam})(\text{CH}_3\text{CN})_2][\text{Ni}(\text{dmit})_2]_2$ (**1**), $[\text{Ni}(\text{NMe}_2\text{-ax-dcyclam})][\text{Ni}(\text{dmit})_2]_2$ (**2**), and $[\text{Ni}(\text{NMe}_4\text{-dcyclam})][\text{Ni}(\text{dmit})_2]_2$ (**3**), respectively. In these complex salts, the cationic complex **I** adopted an octahedral six-coordination geometry with two molecules of acetonitrile occupying the trans coordination sites (structure **A**), while those of complexes **II** and **III** adopted a square-planar four-coordination geometry (structure **B**). The Ni–Ni distances between cation and anion in structure **B** were shorter than those of structure **A**. In the IR spectra, $\nu(\text{C}=\text{S})$ of structure **B** was observed 10 cm^{-1} higher than that of structure **A**, and only in compound **2**, $\nu(\text{C}=\text{C})$ was split at 1346 and 1323 cm^{-1} . Electric conductivities of compounds **1–3** were about 10^{-6} S cm^{-1} at room temperature behaving as semiconductors.

For a decade or so, the metal complexes with the ligand dmit ($2\text{-thioxo-1,3-dithiole-4,5-dithiolato}$), especially the nickel complex, have attracted particular interest of the researchers. Since 1990, over 200 publications have appeared involving derivatives of $[\text{Ni}(\text{dmit})_2]^{n-}$ ($0 < n < 2$). This explosion of interest is attributable to the discovery that certain salts of $[\text{Ni}(\text{dmit})_2]^{n-}$ are electronically metallic.¹ In addition, some salts of $[\text{M}(\text{dmit})_2]^{n-}$ ($\text{M} = \text{Ni}$ and Pd) were found to be superconductors.^{2–7} They are the only transition-metal complexes that have been found to exhibit this property. These remarkable electronic properties owe much to the sulfur-rich molecular structure of the complex, which endows the complexes the strong inter-molecular stacking interactions between the molecular orbitals on sulfur atoms.

Recently, Akutagawa and Nakamura used crown ether complexes as the counter-cations for $[\text{Ni}(\text{dmit})_2]$ salts.⁸ Monovalent M^+ -(crown ether) units were effective in modulating the π – π stacking mode and the lateral S–S interaction of the partially charge-transferred $[\text{Ni}(\text{dmit})_2]^{n-}$ molecules. In the salts of the sandwich-type $[\text{K}(12\text{-crown-4})_2]^+$ and the planar, disc-shaped $[\text{K}(18\text{-crown-6})]^+$, $[\text{Ni}(\text{dmit})_2]$ was found to form dimers and trimers, respectively. Furthermore, the ionic channels, formed by the regular arrays of crown ethers, coexisted with the uniform and highly electronically conducting $[\text{Ni}(\text{dmit})_2]$ stacks of $[\text{Li}_{0.6}(15\text{-crown-5})][\text{Ni}(\text{dmit})_2]_2 \cdot (\text{H}_2\text{O})$ and $[\text{M}_x(18\text{-crown-6})][\text{Ni}(\text{dmit})_2]_2$ ($\text{M} = \text{Li}$, Na , and Cs).⁹ Besides crown ether cations, the complex salt $[\text{Cu}(\text{cyclam})(\text{CH}_3\text{CN})_2][\text{Ni}(\text{dmit})_2]_2$ ($\text{cyclam} = 1,4,8,11\text{-tetraazacyclotetradecane}$) has been prepared, and its crystal structure and the magnetic properties

have been studied by Oshio.¹⁰ In the complex, $[\text{Cu}(\text{cyclam})(\text{CH}_3\text{CN})_2]^{2+}$ had an axially distorted octahedral coordination geometry, where two acetonitrile molecules coordinate to the copper atom at apical coordination sites.

Since we possess a special series of metal complexes ligated with cyclam derivatives, this report inspired us to examine the possible changes brought about by using our series. In this paper, the complex salts of cyclam complex derivatives and $[\text{Ni}(\text{dmit})_2]^-$ were prepared and characterized by electric conductivity and IR spectroscopy. Structural formulae of cyclam derivatives studied in this work are shown in Fig. 1. Complex **III** is the fully *N*-substituted analogue of **I**, synthesised by the alkylation of **I**. In a previous report,¹¹ diastereomeric complexes with cyclam derivatives **I** and **II** were obtained just by changing the order of the reduction and complexation reactions, after macrocycle formation (Curtis-type reaction) of methyl vinyl ketone and *N*-methylethylenediamine. The signif-

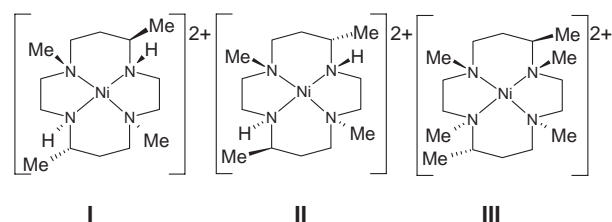


Fig. 1. Structural formulae of $[\text{Ni}(\text{NMe}_2\text{-dcyclam})]^{2+}$ **I**, $[\text{Ni}(\text{NMe}_2\text{-ax-dcyclam})]^{2+}$ **II**, and $[\text{Ni}(\text{NMe}_4\text{-dcyclam})]^{2+}$ **III**.

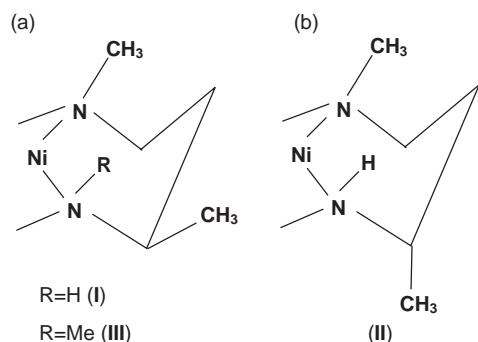


Fig. 2. Conformation of 6-membered ring (a) C-equatorial and (b) C-axial conformation.

icant difference between complexes **I** and **II** is the orientations of two C-methyl groups, i.e., two methyl groups are axial in complex **II** while equatorial in complex **I** as shown in Fig. 2. The axial C-methyl groups and N-methyl groups stick out nearly perpendicular to the NiN₄ plane in complex **II**, Fig. 2b, and strongly interfere with the approach of solvents or other ligands to the apical coordination sites. This is also the case in complex **III**, where four N-methyl groups cause interference. The structures and IR spectra of these complex salts are compared with other reported salts of [Ni(dmit)₂][−].

Experimental

Materials. The complexes of tetra-aza macrocycles **I–III** were synthesised by published procedures.¹¹ However, purification of complex **III** with sephadex C-25 ion-exchange column with the use of 0.2 M NaCl aq was needed to separate the isomers. These three cyclam derivatives are *meso* type. The formation and the purity of the complexes were confirmed by elemental analysis. [Ni(NMe₂-dcyclam)](ClO₄)₂ (**I**): Anal. Found: C, 32.56; H, 6.21; N, 10.65%. Calcd for C₁₄H₃₂Cl₂N₄NiO₈: C, 32.70; H, 6.25; N, 10.90%. [Ni(NMe₂-ax-dcyclam)](ClO₄)₂ (**II**): Anal. Found: C, 32.56; H, 6.16; N, 10.80%. Calcd for C₁₄H₃₂Cl₂N₄NiO₈: C, 32.70; H, 6.25; N, 10.90%. [Ni(NMe₄-dcyclam)(H₂O)₂](Cl₂·4H₂O) (**III**): Anal. Found: C, 36.53; H, 9.86; N, 10.44%. Calcd for C₁₆H₄₈Cl₂N₄NiO₆: C, 36.80; H, 9.27; N, 10.73%. (Bu₄N)[Ni(dmit)₂] was also synthesised by the reported procedures.¹² (NBu₄)[Ni(dmit)₂]: Anal. Found: C, 38.07; H, 5.02; N, 2.15%. Calcd for C₂₂H₃₆N₅S₁₀Ni: C, 38.07; H, 5.22; N, 2.01%. IR: ν_{max}/cm^{−1} 2955(C–H), 1348(C=C), 1058(C=S). All other reagents were commercially available and used without further purifications.

Synthesis of Complex Salts of [Ni(dmit)₂][−] and Nickel Complex of Cyclam Derivatives. Single crystals of compound **1** were prepared by cation-exchange via slow inter-diffusion in acetonitrile:DMF = 10:1 mixed solvent solution (50 mL) of (Bu₄N)[Ni(dmit)₂] (0.1 mmol, 0.069 g) and [Ni(NMe₂-dcyclam)](ClO₄)₂ (0.1 mmol, 0.051 g) for a week at room temperature. Yield, 0.040 g (31%). Anal. Found: C, 28.12; H, 2.43; N, 6.60%. Calcd for C₃₀H₃₈N₆S₂₀Ni₃: C, 27.83; H, 2.47; N, 6.49%. Single crystals of compounds **2** and **3** were similarly prepared using **II** and **III** respectively. **2**: Yield, 0.035 g (28%). Anal. Found: C, 25.74; H, 1.96; N, 4.63%. Calcd for C₂₆H₃₂N₄S₂₀Ni₃: C, 25.64; H, 2.65; N, 4.64%. **3**: Yield, 0.050 g (40%). Anal. Found: C, 26.92; H, 2.53; N, 4.44%. Calcd for C₂₈H₃₆N₄S₂₀Ni₃: C, 26.97; H, 2.89; N, 4.49%.

Measurements. The IR spectra (KBr pellets) were measured using a JASCO FT/IR-410 spectrophotometer, with a resolution of 4 cm^{−1}. Elemental analyses were performed by using a

Perkin-Elmer 2400II CHN Analyzer. Conductivity measurements were carried out at ambient pressure and room temperature using the two-probe method on compacted pellets prepared from powder samples of compounds **1–3**.

X-ray Crystallography. A single crystal suitable for X-ray diffraction study was mounted on a glass capillary, transferred to a Bruker AXS SMART diffractometer equipped with CCD area detector and MoKα (λ = 0.71073 Å) radiation, and centered in the beam at 297 K. The structures were solved and refined with the SHELX-97¹³ using direct method and expanded using Fourier techniques. The number of different Fourier peaks was reduced to recognize the complex molecules. When searching for the methyl groups, it became clear that the macrocycle ligands of complexes **I** and **II** were disordered. Finally, both disorder types were refined with the PART instruction of SHELXL-97. The macrocycle ligand of complex **I** shows disorder in which two sets of positions (C9A/C11A/C12A/C13A and C9B/C11B/C12B/C13B) were located, and that of complex **II** shows disorder in which two sets of positions (C7A/C8A/C9A/C10A/C11A/C12A/C13A and C7B/C8B/C9B/C10B/C11B/C12B/C13B) were located. The occupancies of sites A and B in complex **I** converged at 69.4 and 30.6%, respectively, and the occupancies of sites A and B in complex **II** converged at 50.6 and 49.4%, respectively. All non-hydrogen atoms were refined anisotropically and hydrogens isotropically. Crystal data and selected bond lengths are summarised in Tables 1 and 2, respectively. Crystallographic data have been deposited with Cambridge Crystallographic Data Centre: Deposition numbers CCDC-285399–285401 for compounds **1–3**, respectively. Copies of the data can be obtained free of charge via <http://www.ccdc.cam.ac.uk/conts/retrieving.html> (or from the Cambridge Crystallographic Data Centre, 12, Union Road, Cambridge, CB2 1EZ, UK; Fax: +44 1223 336033; e-mail: deposit@ccdc.cam.ac.uk).

Results and Discussion

Crystal Structure of Complex Salts. ORTEP drawings of disorder pair of NMe₂-dcyclam complex and [Ni(dmit)₂][−] for compound **1** are shown in Fig. 3. The atom numbering was kept consistent in compounds **1–3** except for the additional N-methyl group of complex **III**. The asymmetrical units of all compounds consisted of independent half cation and one anion unit. The nickel atom on the inversion centre was coordinated in distorted octahedral fashion (structure **A**) by four nitrogen atoms from NMe₂-dcyclam ligand and two nitrogen atoms from acetonitriles, which occupy the planar and apical sites, respectively. Bond lengths between nickel ion and donor atoms, given in Table 2, closely resembled those of [Ni(cyclam)(CH₃CN)₂][Ni(dmit)₂]₂, in which the corresponding bond lengths being 2.060(6)–2.065(7) and 2.137(5) Å, respectively, reported by Oshio.¹⁰ The axial Ni–N bond of complex **I** was tilted 2.6° from the normal direction of the NiN₄ plane. The NiS₄ coordination geometry of Ni(dmit)₂ was slightly distorted from square planar toward a tetrahedral configuration, where the twist between the planes S4–Ni1–S5 and S6–Ni1–S7 was 3.2°. The molecular bending at the S1–Ni1–S10 angle of 4.0° was also found for Ni(dmit)₂. The Ni–Ni separation between [Ni(NMe₂-dcyclam)]²⁺ and [Ni(dmit)₂][−] was 5.8539(8) Å, which was longer than that of [Ni(cyclam)(CH₃CN)₂][Ni(dmit)₂]₂, due to the steric hindrance of C-methyl groups (C13), apparent in Fig. 3. As shown in Fig. 4, the crystal structure of compound **1** consisted of anion layers and cation layers

Table 1. Crystallographic Data of Complex Salts **1–3**

		1	2	3
Formula		C ₃₀ H ₃₈ N ₆ Ni ₃ S ₂₀	C ₂₆ H ₃₂ N ₄ Ni ₃ S ₂₀	C ₂₈ H ₃₆ N ₄ Ni ₃ S ₂₀
Fw		1299.99	1217.89	1245.94
Crystal system		Triclinic	Triclinic	Triclinic
Space group		<i>P</i> $\bar{1}$	<i>P</i> $\bar{1}$	<i>P</i> $\bar{1}$
Unit cell	<i>a</i> /Å	9.5011(13)	9.2398(7)	8.9982(6)
	<i>b</i> /Å	11.6082(16)	10.7367(8)	10.8182(7)
	<i>c</i> /Å	12.5764(17)	11.8276(9)	11.9487(8)
	α /deg	75.115(3)	78.218(2)	76.1550(10)
	β /deg	87.183(3)	78.257(2)	82.1410(10)
	γ /deg	67.636(2)	82.006(2)	82.3250(10)
Volume/Å ³		1237.9(3)	1118.76(15)	1112.57(13)
<i>Z</i>		1	1	1
<i>D</i> _{calcd} /Mg m ^{−3}		1.744	1.808	1.86
GOF ^{a)}		0.885	0.91	0.932
Final <i>R</i>		0.0482	0.0338	0.0309
indices [<i>I</i> > 2σ(<i>I</i>)]		0.1014	0.0796	0.0713
<i>R</i> indices		0.0918	0.0501	0.0388
(all data)		0.1138	0.0849	0.0743

a) Goodness-of-fit on F^2 . b) $R_1 = \Sigma||F_o| - |F_c||/\Sigma|F_o|$. c) $wR_2 = \Sigma[w(F_o^2 - F_c^2)^2]/\Sigma[w(F_o^2)^2]^{1/2}$.

Table 2. Selected Bond Lengths (Å)

1		2		3	
Ni(1)–S(4)	2.1616(13)	Ni(1)–S(4)	2.1623(7)	Ni(1)–S(4)	2.1617(6)
Ni(1)–S(5)	2.1535(13)	Ni(1)–S(5)	2.1573(8)	Ni(1)–S(5)	2.1607(6)
Ni(1)–S(6)	2.1574(13)	Ni(1)–S(6)	2.1705(8)	Ni(1)–S(6)	2.1631(6)
Ni(1)–S(7)	2.1536(12)	Ni(1)–S(7)	2.1587(7)	Ni(1)–S(7)	2.1746(6)
Ni(2)–N(1)	2.108(4)	Ni(2)–N(1)	1.949(3)	Ni(2)–N(1)	1.9652(17)
Ni(2)–N(2)	2.086(4)	Ni(2)–N(2)	1.937(3)	Ni(2)–N(2)	2.007(2)
Ni(2)–N(3)	2.141(4)				
S(1)–C(1)	1.625(5)	S(1)–C(1)	1.646(3)	S(1)–C(1)	1.640(2)
S(10)–C(6)	1.635(5)	S(10)–C(6)	1.651(3)	S(10)–C(6)	1.651(2)
C(2)–C(3)	1.361(6)	C(2)–C(3)	1.356(4)	C(2)–C(3)	1.367(3)
C(4)–C(5)	1.353(6)	C(4)–C(5)	1.346(4)	C(4)–C(5)	1.362(3)

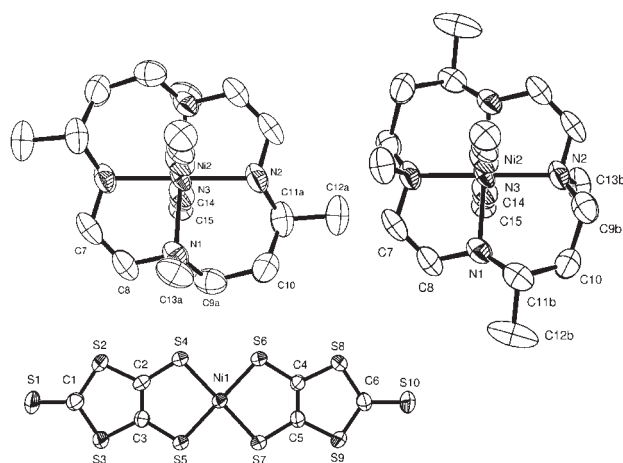


Fig. 3. ORTEP drawing for cation and anion in **1**. Disorder pairs of C9a–C11a–C12a–C13a and C9b–C11b–C12b–C13b are represented and viewed from the same direction. Displacement ellipsoids are drawn at the 50% probability level and the H atoms of the cation part have been omitted for clarity.

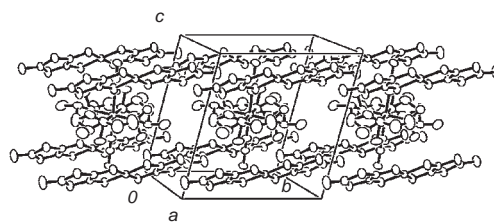


Fig. 4. Crystal structure of **1**, showing the layered structure.

piled up alternately along *c*-axis.

The coordination geometry of complexes **II** and **III** was similar, and the cations adopted square-planar geometry (structure **B**) as shown in Figs. 5 and 6, respectively. Although the crystals were prepared under same conditions as compound **1**, acetonitrile molecules did not coordinate to complexes **II** and **III**. In compound **2**, however, NMe₂-ax-dcyclam complex **II** was disordered as in Fig. 5. Ni2–N bond distances were shorter than those of structure **A**, which was usually the case when the coordination number decreased. In complex **2**, the NiS₄ coordination geometry of Ni(dmit)₂ was essentially pla-

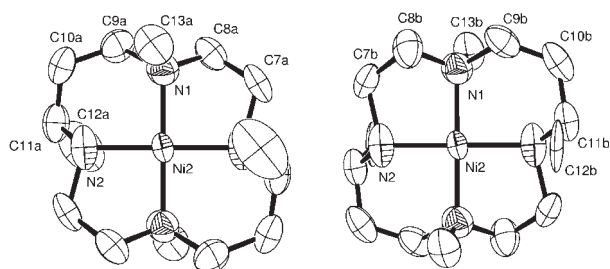


Fig. 5. ORTEP drawing for cation in **2**. Disorder pairs of C7a–C8a–C9a–C10a–C11a–C12a–C13a and C7b–C8b–C9b–C10b–C11b–C12b–C13b are represented and viewed from the same direction. Displacement ellipsoids are drawn at the 50% probability level and the H atoms have been omitted for clarity.

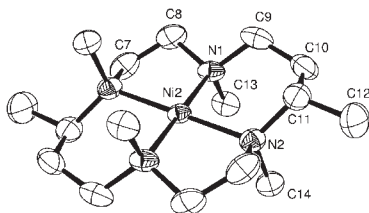


Fig. 6. ORTEP drawing for cation in **3**. Displacement ellipsoids are drawn at the 50% probability level and the H atoms have been omitted for clarity.

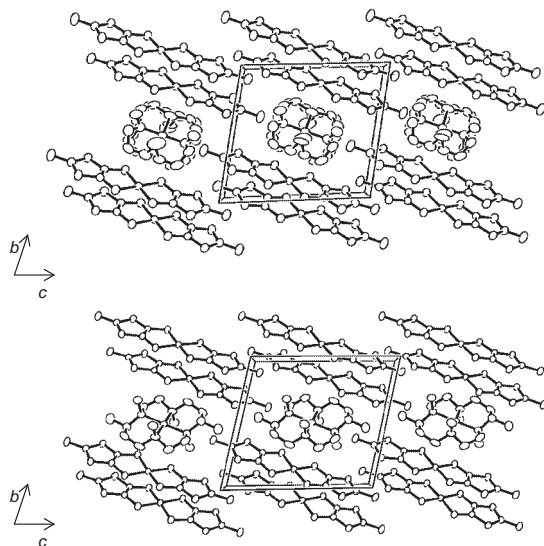


Fig. 7. Crystal structures of **2** and **3** viewed along *a*-axis.

nar, while in **3**, it was slightly distorted from square planar toward a tetrahedral configuration, with the twist between the S4–Ni1–S5 and S6–Ni1–S7 planes being 7.3°. As is shown in Fig. 7, the crystal structures of compounds **2** and **3** consisted of anion layers and cation layers also piled up alternately along the *b*-axis. Ni–Ni separations in compounds **2** and **3** between the cation and the anion were 4.6792(4) and 4.7463(4) Å, respectively, and are shorter than those of [Ni(cyclam)(CH₃CN)₂][Ni(dmit)₂]₂¹⁰ and complex **1**. As was predicted, axially oriented *C*-methyl and *N*-methyl groups in complexes **II** and **III** effectively blocked the coordination of acetonitrile molecules. As can be seen in Fig. 5, the axially oriented *C*-methyl

Table 3. Intermolecular S–S Contacts (Å) Shorter than 3.7 Å^{a)}

1		
S1–S8	3.601(2)	$x, -1 + y, z$
S2–S9	3.410(2)	$1 + x, -1 + y, z$
S3–S8	3.399(2)	$x, -1 + y, z$
S7–S9	3.630(2)	$1 - x, 2 - y, -z$
S9–S9	3.282(3)	$1 - x, 2 - y, -z$
2		
S1–S8	3.560(1)	$x, y, 1 + z$
S1–S9	3.662(1)	$1 - x, -y, 1 - z$
S3–S8	3.371(1)	$x, y, 1 + z$
S3–S10	3.625(1)	$x, y, 1 + z$
S9–S9	3.259(1)	$1 - x, 1 - y, -z$
S9–S10	3.576(1)	$1 - x, 1 - y, -z$
3		
S1–S9	3.455(1)	$x, y, -1 + z$
S2–S9	3.328(1)	$x, y, -1 + z$
S2–S10	3.598(1)	$x, y, -1 + z$
S5–S5	3.551(1)	$1 - x, 2 - y, 1 - z$
S8–S8	3.278(1)	$-x, 1 - y, 2 - z$
S8–S10	3.558(1)	$-x, 1 - y, 2 - z$

a) Symmetry operation applied on second atom.

(C12) groups together with the *N*-methyl (C13) groups of cation **II** are sticking out towards apical coordination sites. A similar situation applies for the *N*-methyl groups C13 and C14 of cation **III** shown in Fig. 6.

In a series of [Ni(dmit)₂]^{*n*−}, intramolecular bond distances reflect the electronic state of the complex. The Ni–S bond distances in compounds **1–3** were in a good accord with those of [N(C₄H₉)₄][Ni(dmit)₂]₂¹⁴ which has been regarded as a monoanion radical. Thus, the [Ni(dmit)₂] moieties in compounds **1–3** were concluded to be monoanionic.

A number of S–S contacts that give rise to possible overlap of the molecular orbitals between different anionic units existed. In Table 3, these intermolecular S–S contacts have been tabulated. The intermolecular interaction of [Ni(dmit)₂][−] predominantly contained the sulfur atoms of thiol groups (S2, S3, S8, and S9) and terminal thioxo groups (S1 and S10) and arrayed as shown in Fig. 8a in each compound. In the case of compound **1**, thiole–thiolato (S9–S7) contact was also present at an opposing site, so that [Ni(dmit)₂][−] complexes were connected by S–S contact. The connection propagated two dimensionally over the entire *ab* plane, which is similar to K(dibenzo-18-crown-6)[M(dmit)₂](CH₃CN)₂ (M = Ni and Au).¹⁵ In the crystal structure of the complex salts with divalent cations, Ca²⁺(DA18-crown-6)[Ni(dmit)₂]₂(CH₃CN)₂ and Co²⁺(15-crown-5)[Ni(dmit)₂]₂(CH₃CN)₂ (DA18-crown-6 = 1,10-diaza-18-crown-6), the long axes of [Ni(dmit)₂][−] anions within the same plane were parallel while that with the next layer were orthogonal to each other. These structures were different from those of compounds **1–3**.¹⁶

In compound **2**, on the other hand, [Ni(dmit)₂][−] unit formed a stacked dimer conformation contacted with an S–S distance of 3.7 Å, shown in Fig. 8b, similar to {[K(18-crown-6)]₂–

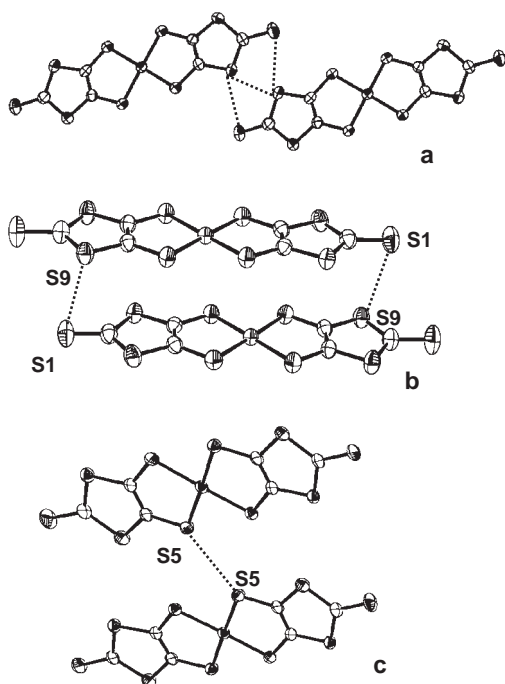


Fig. 8. The interaction shown in **a** were found in all compounds. Stacked dimer (**b**) and side-to-side position pair (**c**) of the $[\text{Ni}(\text{dmit})_2]^-$ units are in **2** and **3**, respectively. Dotted lines indicate the S–S contacts.

$(\text{C}_2\text{H}_4\text{Cl}_2)\{\text{Ni}(\text{dmit})_2\}_2$.¹⁷ Although the crystal structure of compound **3** was similar to that of complex **2** as a whole, there was a slight difference in the S–S contact modes. In compound **3**, $[\text{Ni}(\text{dmit})_2]^-$ complexes were connected by side-to-side S–S contact $\{3.551(1) \text{ \AA}\}$, as shown in Fig. 8c, similar to $\text{Gd}_2(18\text{-crown-6})_2(\text{OH})_2(\text{CH}_3\text{CN})_2[\text{Ni}(\text{dmit})_2]_2$.¹⁸ These S–S contacts in compounds **2** and **3** formed a two-dimensional network in *bc* and (111) planes, respectively. The part of $[\text{Ni}(\text{dmit})_2]^-$ without terminal sulfur atom closed each other, due to the lack of the apical coordination of acetonitrile molecules.

Compounds **1–3** were found to behave as semiconductors in the temperature range of -5 to 100°C , exhibiting room-temperature conductivities of 5.9×10^{-6} , 2.3×10^{-6} , and $3.1 \times 10^{-6} \text{ S cm}^{-1}$, respectively. The two-dimensional conduction paths through the S–S contacts give to the conductive behavior.

IR Spectra. The IR spectra of compounds **1–3** are given in Fig. 9. The absorption peaks around 1050 and 1353 cm^{-1} were assigned to the C=S and C=C stretching vibrations of $[\text{Ni}(\text{dmit})_2]^-$, respectively. In the spectra of compounds **2** and **3** which adopt structure **B**, $\nu(\text{C}=\text{S})$ were shifted to higher wavenumber by 10 cm^{-1} from the general wavenumber of monovalent $\text{Ni}(\text{dmit})_2$, which was the case in compounds **1**.

However, the C=S bond lengths in compounds **2** and **3** were found to be longer than those in complex **1**, Table 2. Additionally, inter-anion interactions of terminal thioxo-sulfur atoms (S1 and S10) of $[\text{Ni}(\text{dmit})_2]^-$ through, the number of S–S contacts in compounds **2** and **3** was greater than that in compound **1** as shown in Table 3. If the C=S bonds were elongated and thus, weakened due to this intermolecular interaction at terminal thioxo-sulfur atoms, $\nu(\text{C}=\text{S})$ should shift to a lower wavenumber. Therefore, the observed $\nu(\text{C}=\text{S})$ shift cannot be ex-

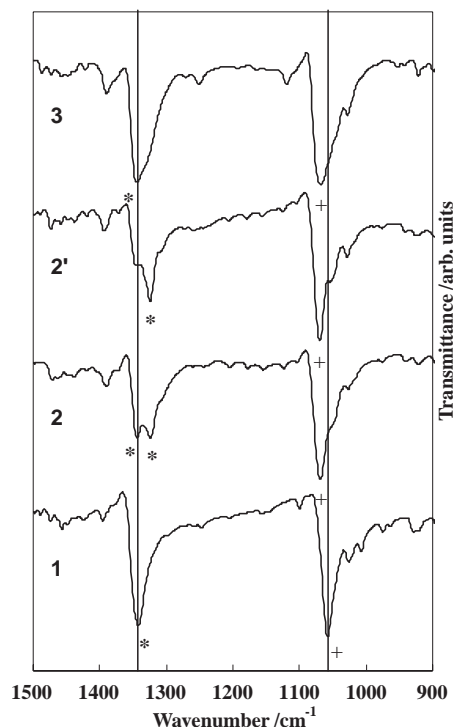


Fig. 9. IR spectra of compounds **1–3**. The spectrum of **2'** was obtained with KBr pellet chilled by liquid nitrogen. The bands indicated with (*) and (+) correspond to $\nu(\text{C}=\text{C})$ and $\nu(\text{C}=\text{S})$, respectively.

plained by this inter-molecular interaction. Morita et al. reported the $\nu(\text{C}=\text{S})$ shift ($1052\text{--}1064 \text{ cm}^{-1}$) in the LB films of $2\text{C}_{18}\text{-Au}(\text{dmit})_2$ which depended on the temperature ($30\text{--}100^\circ\text{C}$). However, they have not clarified the reason of the shift.¹⁹ The structural difference of **A** and **B** is a possible reason for the shift in $\nu(\text{C}=\text{S})$. Recently, we have prepared $(\text{C4Q})_2[\text{Ni}(\text{dmit})_2]$, $(\text{C5Q})_2[\text{Ni}(\text{dmit})_2]$, and $(\text{C9Q})_2[\text{Ni}(\text{dmit})_2]$ ($\text{C4Q} = N\text{-butylquinolinium}$, $\text{C5Q} = N\text{-pentylquinolinium}$, and $\text{C9Q} = N\text{-nonylquinolinium}$) and characterized them with X-ray crystal structural analysis and IR spectroscopy. In this work, a high frequency shift of the C=C and C=S stretching vibration mode was observed depending on the distance between the cationic nitrogen atom and the Ni atom of $[\text{Ni}(\text{dmit})_2]^{2-}$.²⁰ The electrostatic influence of the square-planar four-coordination complex towards $[\text{Ni}(\text{dmit})_2]^-$ estimated to be stronger than that of the octahedral six-coordination one, which might explain the high-frequency shift.

Only in compound **2**, a split of $\nu(\text{C}=\text{C})$ into two peaks at 1346 and 1323 cm^{-1} was observed. A strong band around 1353 cm^{-1} corresponds to the C=C stretching band of mono-anion, and this peak known to exhibit large shifts in relation to the formal charge of $\text{Ni}(\text{dmit})_2$: 1260 cm^{-1} for $[\text{Ni}(\text{dmit})_2]$ ^{0,29} and 1440 cm^{-1} for $[\text{Ni}(\text{dmit})_2]^{2-}$.²¹ This was the first time that a split in the $\nu(\text{C}=\text{C})$ peak. C=C bond lengths of compounds **1–3** given in Table 2 exhibited no apparent change. The only difference between compound **2** and other salts was that the $[\text{Ni}(\text{dmit})_2]^-$ units formed a stacked dimer with a S–S contact distance of $3.662(1) \text{ \AA}$. However, the $[\text{Ni}(\text{dmit})_2]^-$ unit also formed a stacked dimer a S–S distance of 3.7 \AA in complex salts of $4\text{-[2-(4-pyridyl)ethenyl]pyridinium}$, but its $\nu(\text{C}=\text{C})$

stretch was not split.²² In κ -(BEDT-TTF)₂Cu[N(CN)₂]₂Br, a Raman-active EMV-coupled (EMV = electron molecular vibration) ν_3 mode near 1420 cm^{−1} was found, and it exhibited a large low-frequency shift because of the inter-dimer EMV interaction.²³ Furthermore the ν (C=C) of compound **2** was found to exhibit clear temperature dependence. From measurements performed soon after immersing the KBr pellet of compound **2** in liquid nitrogen for 5 min, the lower wavenumber peak remained unchanged while the higher one decreased. This was a reversible phenomenon and compounds **1** and **3** did not exhibit such a spectral change. From this result, the phenomenon was explained by the increase in inter-dimer interaction by decreasing the temperature, due to a decrease in the lattice volume by stopping thermal vibration.

Conclusion

We have prepared three complex salts composed of [Ni(dmit)₂][−] and Ni^{II} cyclam complexes. The cationic complexes of compound **1** adopted octahedral six-coordination geometry with two molecules of acetonitrile occupying the trans coordination sites. The coordination geometry of the cyclam derivatives in compounds **2** and **3** was similar, and the cations adopted square-planar geometry without acetonitrile coordination. The Ni–Ni separations in compounds **2** and **3** between cation complex and anion complex were 4.6792(4) and 4.7463(4) Å, respectively, which are shorter than those of [Ni(cyclam)(CH₃CN)₂][Ni(dmit)₂]₂ and compound **1**. In the IR spectra of compounds **2** and **3**, which adopted structure **B**, ν (C=S) was shifted to higher wavenumber by 10 cm^{−1} from the general wavenumber of monovalent Ni(dmit)₂ due to the electrostatic interaction between the cation and the anion, and in the spectrum for compound **2**, ν (C=C) was split into two peaks (1346 and 1323 cm^{−1}) probably due to [Ni(dmit)₂][−] inter dimer interaction.

References

- 1 P. Cassoux, L. Valade, H. Kobayashi, A. Kobayashi, R. A. Clark, A. E. Underhill, *Coord. Chem. Rev.* **1991**, *110*, 115.
- 2 K. Kajita, Y. Nishio, S. Moriyama, R. Kato, H. Kobayashi, Y. Sasaki, *Solid State Commun.* **1988**, *65*, 361.
- 3 A. Kobayashi, H. Kobayashi, A. Miyamoto, R. Kato, R. A. Clark, A. E. Underhill, *Chem. Lett.* **1991**, 2163.
- 4 H. Kobayashi, K. Bun, T. Nato, R. Kato, A. Kobayashi, *Chem. Lett.* **1992**, 1909.
- 5 M. Bousseau, L. Valade, J.-P. Legros, P. Cassoux, M. Garbaskas, L. V. Interrante, *J. Am. Chem. Soc.* **1986**, *108*, 1908.
- 6 L. Brossard, H. Hurdeamb, M. Ribault, L. Valade, J.-P. Legros, P. Cassoux, *Synth. Met.* **1988**, *27*, 157.
- 7 H. Tajima, M. Inokuchi, A. Kobayashi, T. Ohta, R. Kato, H. Kobayashi, H. Kuroda, *Chem. Lett.* **1993**, 1235.
- 8 T. Akutagawa, T. Nakamura, *Coord. Chem. Rev.* **2000**, *198*, 297.
- 9 T. Nakamura, T. Akutagawa, K. Honda, A. E. Underhill, T. Coomber, R. H. Friend, *Nature* **1998**, *394*, 159.
- 10 H. Oshio, *Inorg. Chem.* **1993**, *32*, 4123.
- 11 K. Miyamura, M. Kohzuki, R. Narushima, M. Saburi, Y. Gohshi, *J. Chem. Soc., Dalton Trans.* **1987**, 3093.
- 12 G. Steimecke, H. J. Sieler, R. Kirmse, E. Hoyer, *Phosphorus Sulfur* **1979**, *7*, 49.
- 13 G. M. Sheldrick, *SHELXS-97 and SHELXL-97, Program for the Solution of Crystal Structures*, University of Göttingen, Germany, **1997**.
- 14 D. Mentzafos, A. Hountas, *Acta Crystallogr., Sect. C* **1988**, *44*, 1550.
- 15 K. Shitagami, T. Akutagawa, T. Hasegawa, T. Nakamura, N. Robertson, *CrystEngComm* **2001**, *3*, 255.
- 16 T. Akutagawa, S. Nishihara, N. Takamatu, T. Hasegawa, T. Nakamura, T. Inabe, *J. Phys. Chem. B* **2000**, *104*, 5871.
- 17 D. Q. Wang, J. M. Dou, M. J. Niu, D. C. Li, Y. Liu, *Acta Chim. Sin.* **2002**, *60*, 2145.
- 18 S. Nishihara, T. Akutagawa, T. Hasegawa, T. Nakamura, *Inorg. Chem.* **2003**, *42*, 2480.
- 19 S. Morita, A. Ikehata, Y. F. Miura, M. Sugi, Y. Ozaki, *Thin Solid Films* **2004**, *464–465*, 408.
- 20 Y. Soneta, J. Iwata, K. Miyamura, in preparation.
- 21 L. Valade, J.-P. Legros, M. Brousseau, P. Cassoux, M. Garbaskas, L. V. Interrante, *J. Chem. Soc., Dalton Trans.* **1983**, 783.
- 22 T. Hirose, H. Imai, T. Naito, T. Inabe, *J. Solid State Chem.* **2002**, *168*, 535.
- 23 M. Maksimuk, K. Yakushi, H. Taniguchi, K. Kanoda, A. Kawamoto, *J. Phys. Soc. Jpn.* **2001**, *70*, 3728.